Colour Coherence in Photon Induced Reactions

A. Lebedev[a], L. Sinclair[b], E. Strickland[b], J. Vazdik[a].

[a] P.N.Lebedev Physical Institute, Academy of Sciences of Russia, Leninsky Prospect 53, 117924 Moscow, Russia
[b] Department of Physics and Astronomy, Glasgow University, G12 8QQ Glasgow, Scotland, U.K.

Abstract: Colour coherence in hard photoproduction is considered using the Monte Carlo event generators PYTHIA and HERWIG. Significant effects in the parton shower are found using multijet observables for direct and resolved photon induced reactions. The particle flow in the interjet region of direct processes shows a strong influence of string fragmentation effects.

1 Introduction

Colour coherence is an intrinsic property of QCD. Its observation is important in the study of strong interactions and in the search for deviations from the Standard Model [1]. It is interesting to look for colour coherence effects in hard photoproduction processes at the ep-collider HERA where large momentum transfers can be achieved and both direct (Fig. 1(a)) and resolved (Fig. 1(b)) photon induced events occur. In Section 2 multijet observables are studied which

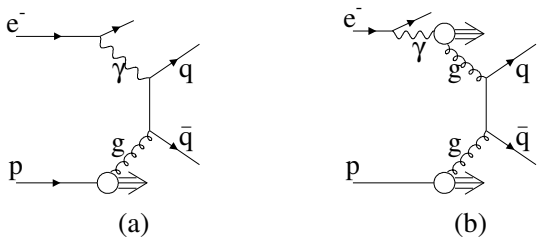

Figure 1: *Examples of (a) direct and (b) resolved photoproduction*

reveal coherence at the parton shower level for both direct and resolved photoproduction. In Section 3 consideration of the particle flow in direct photoproduction shows colour coherence effects at the fragmentation stage of hadron production.

2 Multijet observables

The effects of colour coherence on the emission pattern of jets in e^+e^- collisions are well known and intuitive. However in hadron–hadron collisions the large number of possible colour flows involved in jet production complicates the identification of variables sensitive to coherence.

Here, radiation patterns in γp collisions are studied by considering events where soft radiation is hard enough to form a jet. This reduces the effect of secondary interactions in resolved photoproduction.

The effects arising from different implementations of coherence were studied using 500 pb^{-1} of events generated with PYTHIA 5.7 [2] and HERWIG 5.8 [3]. Direct and resolved events were generated separately and combined according to their cross sections. Events were generated with a minimum p_T of 20 GeV using the GRV proton and photon structure functions [4]. Two event samples were generated using PYTHIA: the PYTHIA Coherent sample and the PYTHIA Incoherent sample which was obtained by switching off the coherence in the parton shower and the initial-final state coherence. HERWIG represents an alternate implementation of coherent processes. Jets of particles were found using the KTCLUS [5] algorithm in covariant p_T mode with radius equal to 1. Three jet events with at least two jets of transverse energy (E_t^{jet}) satisfying $E_t^{jet} > 30$ GeV and a third jet of $E_t^{jet} > 3$ GeV were selected. The jets are ordered by E_t^{jet} decreasing and referred to as "first", "second" and "third" jet acccordingly in the following. Two scenarios were considered, one to reflect the acceptance in jet pseudorapidity (η^{jet}) of the present ZEUS detector, $|\eta^{jet}| < 2.5$, and one to show the possibilities with an extended acceptance, $|\eta^{jet}| < 4$. In addition the events satisfied $0.2 < y < 0.85$ and $P^2 < 4$ GeV^2, where P^2 is the negative of the four-momentum squared of the photon.

An overall drop in cross section is observed between incoherent and coherent event samples. For example, with a luminosity of 250 pb^{-1} and the standard detector acceptance, $|\eta^{jet}| < 2.5$, 2600 multijet events are predicted by PYTHIA Incoherent, 1728 by PYTHIA Coherent and 1665 events by HERWIG. For comparison in the extended acceptance scenario, $|\eta^{jet}| < 4$, 3012 multijet events are predicted by HERWIG.

The angular distribution of the third jet is also affected. Following [6] the angle α is defined as the azimuthal angle of the third jet about the second jet in the $\eta - \varphi$ plane. Here, however, we use centre-of-mass (c.m.) variables so $\alpha = \arctan(\Delta H/|\Delta\varphi|)$ where $\Delta H = \mathrm{sign}(\eta_2^{cm})(\eta_3 - \eta_2)$ and $\eta_2^{cm} = \eta_2 - 1/2(\eta_2 - \eta_1)$ and $\Delta\varphi = \varphi_3 - \varphi_2$. η_1, η_2 and η_3 refer to the pseudorapidities in the lab frame of the first, second and third jets respectively and positive η is in the direction of the incoming proton. $\Delta\varphi$ is the difference in azimuth (φ) between the second and third jets (in radians). The definition of α is illustrated for a typical event geometry in Fig. 2(c). The distribution of α as shown in Fig. 2(a) is broader for coherent events. This is consistent

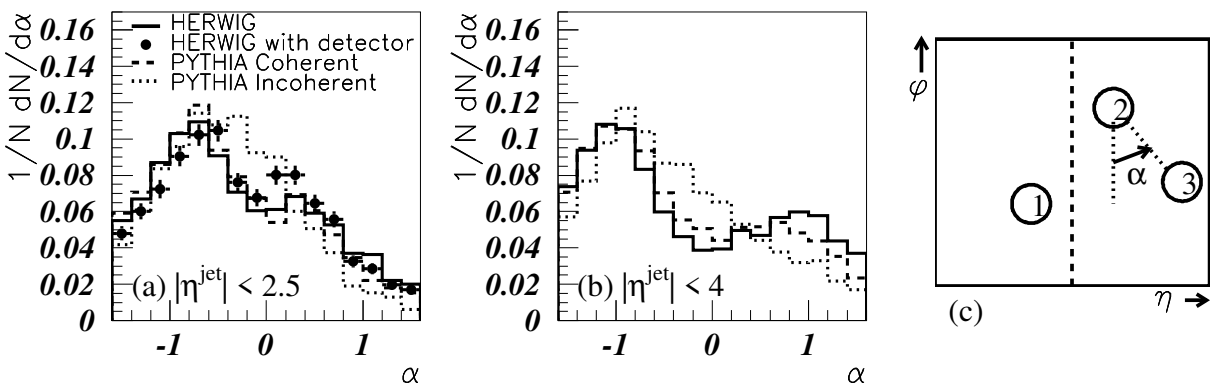

Figure 2: *α distributions (a) with the present acceptance and (b) with extended acceptance. (c) illustrates the definition of α for a typical event geometry. Jets are ordered by E_t^{jet} decreasing.*

with our understanding that for coherent processes radiation is generally suppressed in regions far from the directions of the incoming coloured partons. In addition, reducing the bias on

the distribution by increasing the acceptance from $|\eta^{jet}| < 2.5$ to $|\eta^{jet}| < 4$ produces a more pronounced depletion in the central region for coherent events (Fig. 2(b)).

Canonical detector effects were simulated by smearing the HERWIG jet quantities with Gaussian distributions of varying widths. A resolution of 20% (10%) was used to smear the E_t^{jet} of jets with $E_t^{jet} < 10$ GeV ($E_t^{jet} \geq 10$ GeV). The width of the difference between generated and detected values of η^{jet} and φ^{jet} was taken to be 0.1. As shown in Fig. 2(a) such detector effects should not seriously hinder the measurement of α distributions.

The coherent emission of soft radiation does not have a strong effect on the jet profiles of the first and second jets. For instance, in Fig. 3(a) the transverse energy profile of the second jet is shown. This is the distribution of $\delta\eta_2 = \eta^{part} - \eta_2$, where η^{part} is the η of a particle within

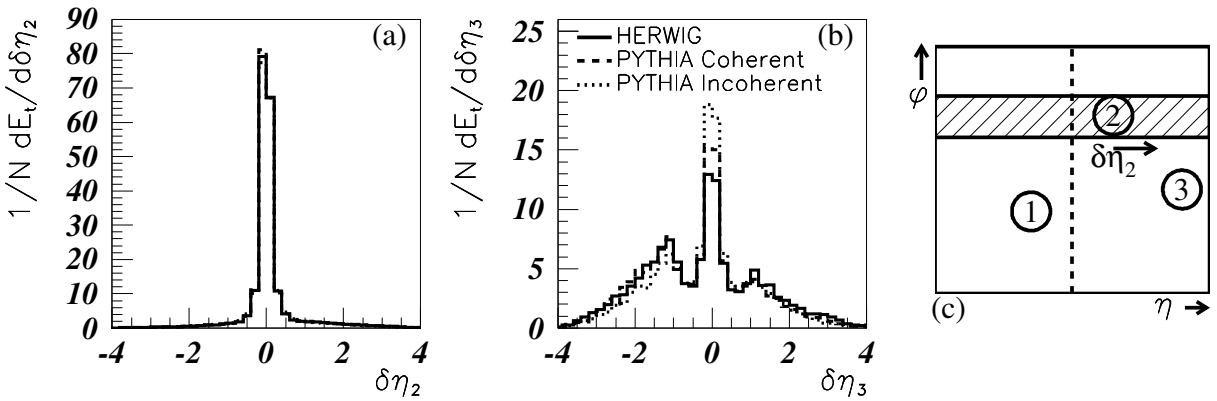

Figure 3: *Jet profiles for (a) the second and (b) the third highest E_t^{jet} jets for the extended acceptance scenario. The definition of the jet profile is illustrated in (c) for the second jet.*

one radian of φ of the jet centre, weighted by the transverse energy of the particle, as illustrated in Fig. 3(c). For this the extended acceptance scenario particles are considered with absolute η up to 5. The profile of the third jet is shown in Fig. 3(b). The occurrence of two peaks outside the jet core is due to partial overlap in φ of the first or second jet. A strong effect of coherence is apparent; it leads to less energy in the core of the third jet.

One of the anticipated effects of colour coherence is that radiation from an incoming parton should be inhibited in regions far from the initial partons direction. Therefore in direct photoproduction events, where the single coloured parton in the initial state has positive η, the coherent emission pattern should be at relatively higher η than the incoherent emission. We have selected a subsample of events which is enriched in direct photon events by requiring $x_\gamma > 0.8$ where $x_\gamma = (\sum_{jets} E_t^{jet} e^{-\eta^{jet}})/(2E_\gamma)$. The sum runs only over the two highest E_T^{jet} jets and E_γ is the energy of the incoming photon. The η of the third jet in the c.m. frame, $\eta_3^{cm} = \eta_3 - 1/2(\eta_2 - \eta_1)$, is shown for this selection in Fig. 4(a). The expected effective enhancement of radiation at large η_3^{cm} can clearly be seen.

Resolved events, with incoming coloured partons from both the γ and p directions, should show an effective enhancement of radiation in coherent processes both at higher positive and at more negative pseudorapidities in comparison to incoherent emission. This effect is evident as shown in Fig. 4(b). Note that the extended acceptance scenario must be employed in order to see the relative enhancement of radiation at high η in resolved events.

To summarize this section, a high integrated luminosity ($\sim 250\text{pb}^{-1}$) is desirable in order to accumulate statistics in multijet events at high E_t^{jet}. However luminosity upgrades which involve a significant reduction of forward acceptance are not worthwhile for this study. They destroy the sensitivity to colour coherence without significantly improving the statistical uncertainty.

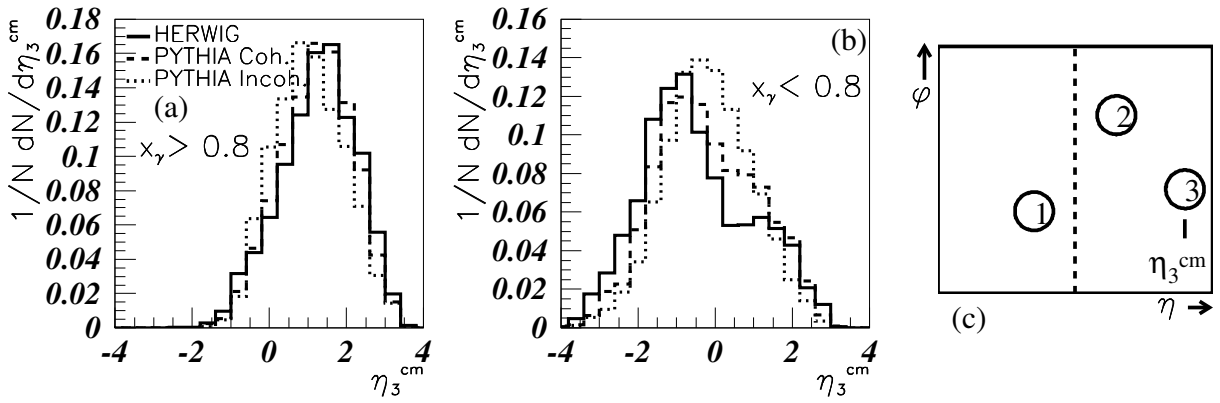

Figure 4: η_3^{cm} *distributions separated by an* x_γ *cut of* 0.8 *into (a) direct and (b) resolved samples for the extended acceptance scenario of* $|\eta^{jet}| < 4$. *In (c) the definition of* η_3^{cm} *is illustrated.*

3 Interjet string effects in direct photoprocesses

Colour coherence effects which lead to a change in particle flow N distributions in the interjet region should be rather pronounced in the direct photon induced processes such as QED Compton on quark (QEDC), QCD Compton (QCDC) and Photon Gluon Fusion (PGF). These distributions are considered here using the PYTHIA [2] generator with string (SF) or independent parton fragmentation (IF) into hadrons. Using SF is equivalent to taking into account the coherence effects at the hadronization phase of event generation. The flow N depends on the string topology and colour antennae which are different for the three direct processes as shown in Fig. 5(left).

The calculation at the generator level was done using the GRV proton structure function [4] and minimum p_T equal to 2.0 GeV. The H1 detector simulation was taken into account as well. A jet-cone algorithm [7] with radius equal to 1 was used for the selection of two jets and gamma-jet events with $E_t^{jet\,or\,\gamma} > 3$ GeV and jet (or final γ) emission angles $25 - 155^o$. This procedure corresponds to the selection of mainly direct processes. The calculated flow of charged particles with $p_t > 0.2$ GeV emitted at angles of less than 20^o to the reaction plane is shown in Fig. 5(right) as a function of the scale angle Ω. Ω is defined [8] as the ratio of the particle angle θ_h to the angle between partons. $\Omega = 0$ corresponds to the direction of the initial state photon; $\Omega = 1$ – the final state quark; $\Omega = -1$ – the final state γ, gluon or antiquark for QEDC, QCDC or PGF respectively; $\Omega = -2$ or 2 – the proton remnant.

It is seen that in the scale angle region between 1 and 2 (region II in Fig. 5) SF (solid histogram, generator level) and IF (dashed histogram, generator level) give different predictions for N. SF taking into account colour forces leads to a suppression of particle flow which is especially strong for QCDC process. The H1 detector simulation (dark circles, SF) weakly distorts the generator level N distribution except for directions close to remnant proton emission where detector acceptance is rather low. Thus colour coherence effects can be observed at the detector level.

It is interesting to consider ratios of particle flows N for different processes since the ratio is less sensitive to experimental errors. The ratios $R = N(QCDC)/N(QEDC)$, $R^* = N(QCDC)/N(PGF)$ are shown in Fig. 6. Fig. 6 displays more clearly the role of colour coherence which leads to drag effects in particle distributions. It is seen that for the case of SF the suppression in N for QCDC is more pronounced than for QEDC and PGF. At $\Omega = 1.7$ the suppression reaches a factor of ~ 3. It has been found that misidentification of quark and

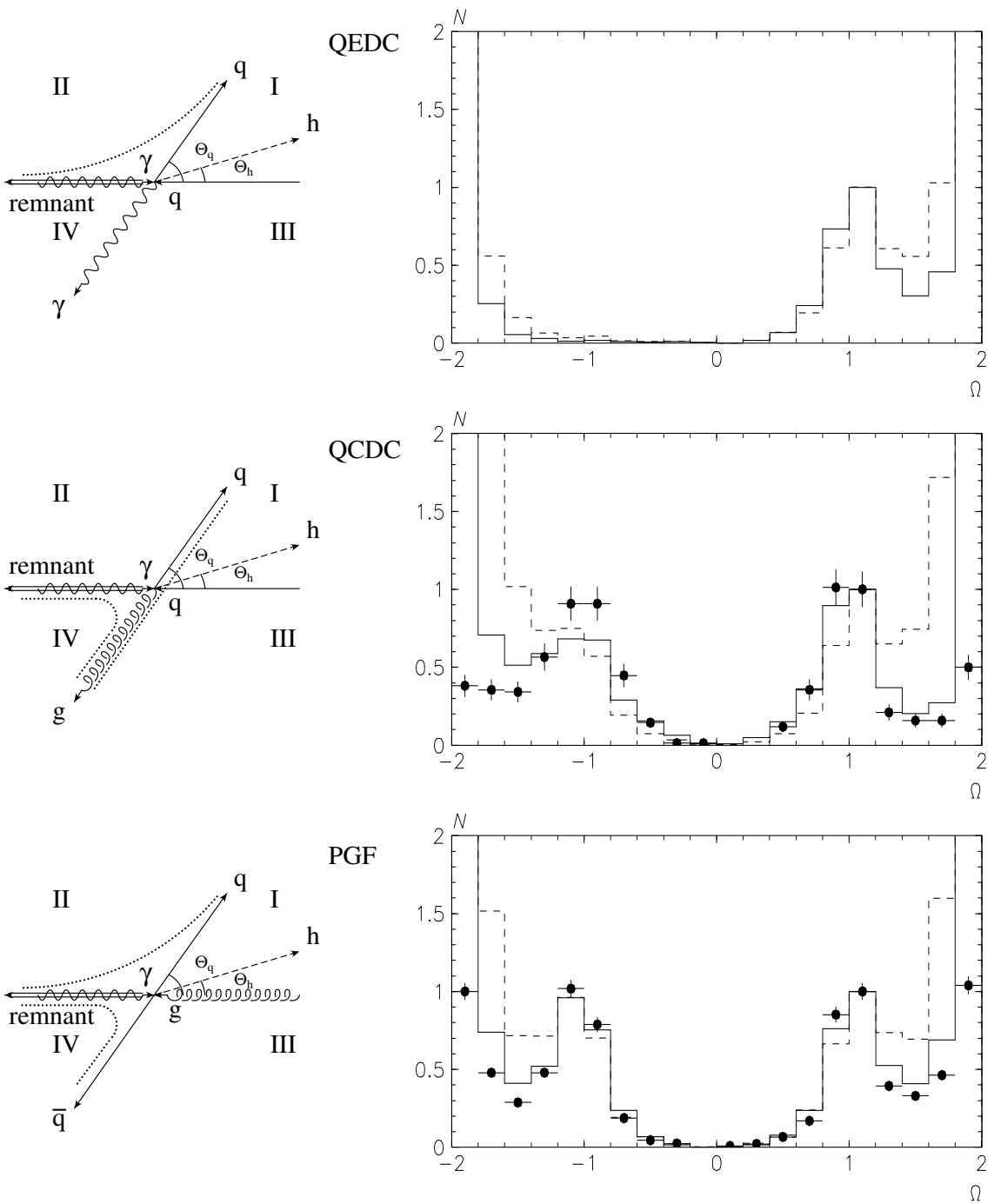

Figure 5: *Left: Topology of direct photoproduction processes in the $\gamma-$parton c.m. frame. The double line is the proton remnant, dotted - strings. θ_q and θ_h are quark and hadron emission angles. Right: Charged particle flow N normalized to 1 at the quark emission angle vs the scale angle Ω. Solid line - generator level SF, dashed line - generator level IF, dark circle - H1 simulation SF. In the regions I - IV Ω is changing within the limits: $0 \leq \Omega \leq 1$ (I), $1 \leq \Omega \leq 2$ (II), $-1 \leq \Omega \leq 0$ (III), $-2 \leq \Omega \leq -1$ (IV).*

gluon jets for QCDC does not change this conclusion.

To observe colour coherence at the fragmentation stage of hadron production in direct processes it is necessary to distinguish these processes from resolved photoproduction and to

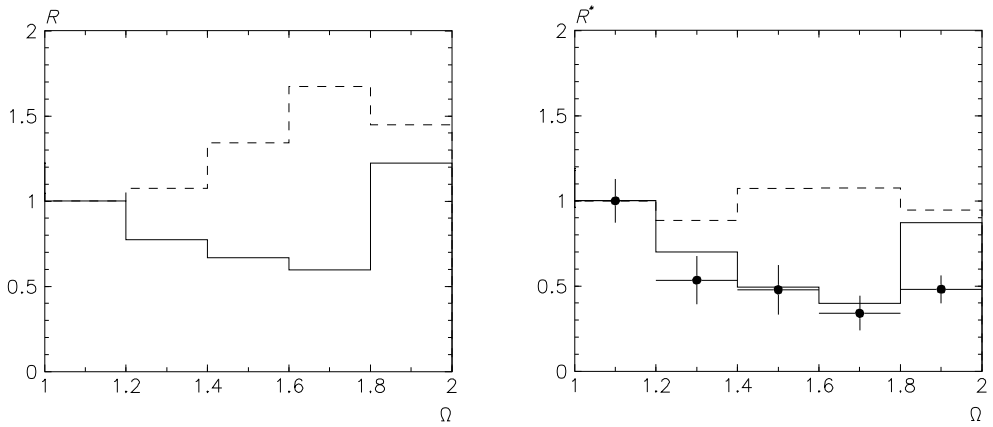

Figure 6: *Ratios R and R^* in the scale angle region $1 < \Omega < 2$. Notations are as in Fig. 5.*

separate QEDC, QCDC and PGF from each other. The jet selection procedure used here enriches the data sample with direct processes. Further enrichment can be achieved by going to larger $E_t^{jet\,\mathrm{or}\,\gamma}$ and by choosing events with x_γ close to 1. Since the direct processes cross section is low we expect ~ 230 QEDC events at the detector level for an integrated luminosity of ~ 100 pb^{-1}. So higher luminosity is needed to study interjet coherence.

4 Conclusions

The observation of colour coherence in photoproduction processes is an important challenge, particularly given the unique opportunity at HERA to study direct as well as resolved photon induced reactions. Since the cross sections of multijet events or of prompt photon reactions are small high luminosity *ep*-collisions are necessary for their study. 250 pb^{-1} would appear to be barely sufficient for these studies; however in upgrading to 1000 pb^{-1} it is essential that the forward acceptance should not be reduced.

References

[1] Yu.L.Dokshitzer, V.A.Khoze, A.H.Mueller and S.I.Troyan, *Basics of Perturbative QCD*, ed. Tran Than Van (Editions Frontières, Gif/Yvette, 1991).

[2] H-U.Bengtsson and T.Sjöstrand, *Computer Phys.Comm.* **46**, 43 (1987); T. Sjöstrand, M.Bengtsson, *Computer Phys.Comm.*, **43**, 367 (1987).

[3] G.Marchesini and B.Webber, *Nucl. Phys. B* **286**, 461 (1988).

[4] M.Gluck, E.Reya, A.Vogt, *Z.Phys. C* **53**, 127 (1992); *Phys. Rev. D* **46**, 1973 (1992).

[5] S.Catani, Yu.L.Dokshitzer, M.H.Seymour and B.R.Webber, *Nucl.Phys. B***406**, 187 (1993).

[6] F.Abe et al, CDF Collaboration, *Phys. Rev. D***50**, 5562 (1994).

[7] J.E.Huth et al, *Fermilab-Conf-90/249-E* (1990).

[8] V.A.Khoze, A.I.Lebedev, J.A.Vazdik, *Mod.Phys.Lett. A* **9**, 1665 (1994).